Title: The Simon effect modulates N2cc and LRP but not the N2pc component.

Authors: [a]Cespón, J., [a]Galdo-Álvarez, S., and [a]Díaz F.

[a]Laboratorio de Neurociencia Cognitiva Aplicada, Facultade de Psicoloxía, Universidade de Santiago de Compostela, 15782 Santiago de Compostela, Galiza, Spain.

Corresponding author: Jesús Cespón

Tel.: +34 981 563100 Ext.: 13732

Fax number: +34 881813901

E-mail addresses:

jesus.cespon@usc.es (Jesús Cespón)

santiago.galdo@usc.es (Santiago Galdo-Alvarez)

fernando.diaz@usc.es (Fernando Díaz)

ABSTRACT:

Previous studies have reported that the horizontal arrangement of the stimuli in Simon tasks elicits three different components: LRP, N2pc and N2cc. Although N2cc may play a key role in Simon tasks, as it is involved in preventing responses based on stimulus position, modulation of the N2cc component according to the experimental condition was not previously investigated because of N2cc/LRP overlap in similar regions and temporal window. The aim of the present study was to investigate how the Simon effect modulates N2pc, N2cc and LRP components. With this purpose, participants had to respond to an arrow according to its colour. Three conditions (depending on the congruency between stimulus position and the required response) were analyzed: compatible position (CP), incompatible position (IP), and neutral position (NP). The LRP peak latency was delayed in IP with respect to CP and NP conditions. Lateralized minus Neutral position (L-NP) subtractions were carried out to remove the common motor activity and isolate the N2cc and N2pc components in the lateralized conditions. The amplitude of N2cc in L-NP waveforms was larger in IP than in CP, in accordance with the greater effort required to monitor the selection of the correct response in the first condition. The eLORETA analysis also revealed more premotor activity between 150-200 ms in IP and CP than in NP, which was attributed to the N2cc component present in IP/CP conditions. Evidence of functional dissociation between N2pc and N2cc components was obtained since N2cc, but not N2pc, was affected by the experimental conditions.

Keywords: Simon effect; event-related potential; spatial attention; premotor cortex; eLORETA.

1. Introduction

The Simon task is a stimulus-response compatibility task (SRC) (Kornblum and Stevens, 2002) in which participants must respond to spatially lateralized stimuli by pressing one of two buttons. The response buttons are also lateralized in the same spatial arrangement as the stimuli, with the position of the stimuli being irrelevant to the task. In those cases in which the required response is on the opposite side to the stimulus (incompatible condition), a type of interference known as the Simon effect is produced (for reviews see Leuthold, 2011; Lu and Proctor, 1995; Simon, 1990). The interference is manifested by a slower reaction time (RT) in the incompatible condition than in the compatible condition in which the response side is ipsilateral with respect to the stimulus position.

The locus of the Simon effect was established in the response selection stage (Valle-Inclán, 1996) through the lateralized readiness potential (LRP). The LRP is an event-related potential (ERP) associated with motor activity that enables distinction between interference produced during motor stages and interference produced during perceptual stages of processing (Gratton et al., 1988; for a review of different ways of obtaining LRP, and its functional significance, see Eimer, 1998). However, it has been shown that the location of the stimuli produces lateralized modulations that overlap with motor activity.

When the stimuli are presented in a horizontal arrangement, the eccentric location induces asymmetry in the exogenous ERP N1 (around 180 ms) (Valle-Inclán, 1996, Experiment 1). This asymmetry can extend to central regions, thus affecting measurement of the LRP. To avoid such asymmetry, some researchers have presented a non-target stimulus in the contralateral hemifield (Valle-Inclán, 1996, Experiment 2). However, such stimulus configuration requires visuospatial selection of the relevant

stimulus, which elicits a component named N2 posterior contralateral (N2pc). N2pc is observed at parieto-occipital electrode sites contralateral to the stimulated hemifield, between 200 and 300 ms, and represents visuospatial processing of the relevant stimulus (Luck and Hillyard, 1994; Woodman and Luck, 1999, 2003). N2pc may be accompanied by a deflection of the same polarity at central electrodes (N2 central contralateral- N2cc), which would hinder evaluation of the motor activity (Valle-Inclán, 1996 Exp. 2; Wascher and Wauschkuhn, 1996). N2cc was proposed to play an important role in preventing cross-talk between the direction of spatial attention and the manual response preparation (Praamstra, 2006; Praamstra and Oostenveld, 2003).

The N2cc wave was first interpreted as volume conduction from posterior areas, i.e. from N2pc activity (Valle-Inclán, 1996 Exp. 2; Wascher and Wauschkuhn, 1996). However several studies evidenced that N2pc and N2cc were different components. Oostenveld et al. (2001), using a biophysical model, showed that the amplitude recorded in central electrodes in the temporal window of the N2pc was too large to be explained through volume conduction from N2pc sources. Also, in the mentioned study, as well as in other studies (Praamstra and Oostenveld, 2003; Praamstra and Plat, 2001), peaks of activity were found at central and at parieto-occipital regions through source reconstruction techniques, indicating the existence of two different components. Moreover, Van der Lubbe et al. (2001) showed that lateralization at central electrodes did not occur parallel to the N2pc, suggesting different sources of activity for central and parieto-occipital waves. Finally, some studies showed a functional dissociation between N2pc and N2cc since both were differentially affected by the experimental manipulations of the tasks (see Praamstra, 2006; Praamstra and Oostenveld, 2003).

The scalp distribution of the N2cc, as well as the conditions under which it was elicited, suggested that N2cc was associated with activation of the dorsal premotor

cortex (dPM) (see Praamstra and Oostenveld, 2003). In fact, the dPM was involved in selection of movements according to learned associations in spatial tasks (Rushworth et al., 2003). Also dPM was considered a region where visual and motor signals interact (Wise et al., 1996; Wise et al., 1997; for a review on dPM, see Abe and Hanakawa, 2009).

In order to prevent overlap between N2pc / N2cc and the motor activity, some researchers have used a vertical arrangement of stimuli and responses (de Jong et al., 1994; Stürmer et al., 2002; Valle-Inclán, 1996, Experiment 3). Using this arrangement, N2cc and N2pc are not elicited. Nonetheless, in our opinion (see also Leuthold, 2011), it is important to examine the N2cc in the Simon task, as it might reflect a mechanism of cognitive control.

The present study involved a Simon task with lateralized stimuli. The positions of the stimuli were compatible (compatible position, CP), incompatible (incompatible position, IP) or central (neutral position, NP) with respect to the required response, and the stimuli were presented in a horizontal arrangement to determine whether the location modulated only motor processes (analyzed via LRP) as maintained in previous studies (de Jong et al., 1994; Stürmer et al., 2002; Valle-Inclán, 1996, Experiment 3) or also other cognitive processes, specifically the visuospatial processing of the relevant stimulus (which has been related to N2pc) and the cognitive control that prevents the execution of the response based on stimulus position (which has been related to N2cc).

In order to clarify the existence of these effects, two procedures were carried out to isolate the N2cc and N2pc components from the motor activity. Firstly, the NP waveform was subtracted from the CP and the IP waveforms, as central stimuli elicit LRP but not N2cc and N2pc components. Also, analyses were carried out in order to discard that the differences in motor activity between lateralized and NP conditions

affected to these Lateralized − Neutral Position (L-NP) waveforms. Secondly, the CP and the IP conditions were compared with the NP condition by means of eLORETA source analyses (Pascual-Marqui, 2007, 2009).

In the waveforms in which N2cc and N2pc were isolated (i.e. when the motor activity is subtracted), we expected to find a larger N2cc amplitude in the IP than in the CP condition, as the cognitive control to monitor the selection of the response based on the relevant dimension (the colour of the arrow) should be greater in the IP than in the CP condition. Using e-LORETA estimations, it was expected to find higher activity on premotor areas during the N2cc time interval in the CP and IP than in the NP. We did not expect to find any differences in the N2pc component between CP and IP, as the Simon effect does not appear to take place in the visuospatial processing of the relevant stimulus. Therefore, another aim of the present study was to provide new evidence of the functional dissociation between N2pc and N2cc components. Finally, with respect to the modulation of the motor activity by the stimulus position, we expected to find longer LRP peak latency in the IP than in the CP and NP conditions consistently with slower RT in the IP condition.

2. Methods

2.1. Participants

Nineteen participants (14 women, 5 men) between 19 and 28 years old (mean age: 21 years old) were recruited from the local university population. Four participants (3 women) were not included in some of the ERP analyses because of an insufficient number of artefact-free epochs in some of the conditions. The participants volunteered to take part in the study and were paid for participating. The study received prior approval by the local ethical review board. Eighteen of the participants were right-handed and one was ambidextrous (evaluated by the Edinburgh Handedness Inventory:

Oldfield (1971)). All participants had normal or corrected to normal vision and none had any history of neurological or psychiatric disorders.

2.2. Stimuli

A series of upward-pointing red or blue arrows was displayed on the screen against a black background, either on the left or on the right side of a white central cross for both compatible and incompatible conditions. In the neutral condition, the stimuli were upward-pointing red or blue arrows placed on the central cross. The arrow stimuli subtended 2.87º x 1.72º (height x width) of the visual field. In the compatible and incompatible conditions, the visual stimuli were presented 3.1 degrees (visual angle) from the centre of the screen at the centre of the stimulus. The lateralized (CP and IP) and central stimuli were presented in parafoveal and foveal regions respectively (see Bargh and Chartrand, 2000), although differences in stimuli processing due to that eccentricity were not expected according to previous studies (Galashan et al., 2008; Mancebo-Azor et al., 2009). In the compatible and incompatible conditions, a geometric figure (two superimposed orthogonal bars, with the vertical bar longer than the horizontal bar, of similar size and eccentric position as the arrow) appeared in the opposite hemifield, with the aim of avoiding exogenous lateralization in the electroencephalogram (EEG) (see Figure 1).

Figure 1 about here

2.3. Procedure

The participants were asked to direct their gaze towards the central cross during the task, and were instructed to respond to the colour of the arrow as quickly as possible by pressing one of the two buttons assigned to each colour. They were also instructed to ignore the position of the arrow. A cross appeared in the centre of the screen and remained in view throughout the task. The two response buttons were arranged

horizontally and were pressed with the corresponding hand (right or left) so that when the arrow was in the central position, there was no overlap between the position and the dimension of the response, and the trials were therefore considered neutral. In each block, each of six possible types of stimuli, grouped in three conditions with the same number of trials (80 per condition) were presented randomly: compatible position (CP, the response required was ipsilateral to the hemifield of appearance of the target), incompatible position (IP, the required response was contralateral to the hemifield of the appearance of the target), and neutral position (NP, as described above, there was no overlap between stimulus position and response). The arrows were presented for 100 ms, with inter-trial intervals of 2000 ms. The short duration of presentation of the stimuli, along with the simultaneous presentation of the non target stimulus in the contralateral hemifield, minimized the probability of ocular movements towards the position of the target when this was presented at eccentric locations (see Abrahamse and Van der Lubbe, 2008).

During the task, participants were seated in a comfortable chair in a dimly lit, sound-attenuated, electrically shielded chamber. The experiment included a practice block of 16 trials and two experimental blocks of 120 trials each, with a resting interval of 90 s between blocks.

The trials were counterbalanced so that half of the participants were instructed to respond by pressing the button on the left with the left hand, in response to the blue arrow, and the button on the right with the right hand, in response to the red arrow, whereas the other participants were given instructions to respond in the opposite way.

2.4. Recordings

Electroencephalographic activity was recorded at 49 active electrode sites, inserted in an electrode cap (Easycap, GmbH) in accordance with the 10-10 International System:

AFz, AF3, AF4, AF7, AF8, Fz, F3, F4, F5, F6, F7, F8, FCz, FC1, FC2, FC3, FC4, FT7, FT8, FT9, FT10, Cz, C1, C2, C3, C4, C5, C6, T7, T8, CPz, CP3, CP4, TP7, TP8, TP9, TP10, Pz, P3, P4, P7, P8, P9, P10, PO7, PO8, Oz, O1 and O2. The EEG signal was passed through a 0.01–100 Hz analogue bandpass filter, and was sampled at 500 Hz. The reference electrode was placed on the tip of the nose and the ground electrode at Fpz. Simultaneously to EEG recordings, ocular movement (EOG) recordings were obtained with two electrodes located supra- and infraorbitally to the right eye (VEOG) and another two electrodes at the external canthus of each eye (HEOG). All impedances were maintained below 10 kΩs. After signal storage, ocular artefacts were corrected off-line by use of the algorithm proposed by Gratton et al. (1983); the EEG was then segmented separately for each condition and manual response (in order to study Lateralized event-related potentials), and 1000-ms epochs (200 ms pre-stimulus baseline) aligned to the onset of stimulus presentation. The signal was passed through a 0.01–30 Hz digital band-pass filter. Epochs with signals exceeding ±100 μV were automatically rejected, and all remaining epochs were inspected individually to identify those still displaying artefacts; the artefacted epochs were also excluded from subsequent averaging. The mean number of epochs (± Standard Deviations) for each condition was the following: Compatible trials: 70 (±8.2); Incompatible trials: 65.7 (±9.9); and Neutral trials 72.67 (±7.7). Epochs were then corrected to the mean voltage of the 200-ms pre-stimulus recording period (baseline).

2.5. Data analysis

Trials with incorrect responses or RTs outside the 100-1000 ms range were considered incorrect and were excluded. The RTs and percentages of incorrect responses were analysed. Interference was considered as the difference between the RT in the IP condition and the RT in the CP condition. To determine if the magnitude of the

interference, or of a possible facilitation, depended on the speed of response, three distributional analyses (DA) of the RTs were carried out (Ratcliff, 1979): IP – CP; IP – NP; and CP – NP. For this, the RTs were ordered on the basis of their speed, and for each participant the RTs at the 4 Quintile Intersection Points that divided the distribution into 5 equal parts (quintiles) were selected.

Lateralized event-related potentials (L-ERPs) were calculated as the differences in contralateral and ipsilateral activation at homologous electrodes (C3/4 for analyses related to the N2cc/LRP complex; P7/8 and PO7/8 for the analyses related to N2pc).

The operation for calculating the N2pc component can be summarized by the formula $[(P7/PO7 - P8/PO8)_{\text{right-hemifield target stimulus}} + (P8/PO8 - P7/PO7)_{\text{left-hemifield target stimulus}}]/ 2$ (see Wascher and Wauschkuhn, 1996). N2pc latency and amplitude were determined as the maximum peak with respect to baseline in the 210-280 ms interval in the CP and IP conditions, based on inspection of the grand average and similar to the temporal window considered by previous reports (e.g. Woodman and Luck, 1999).

The operations for obtaining the N2cc/LRP complex can be summarised by the formula: $[(C4 - C3)_{\text{left-hand movements}} + (C3 - C4)_{\text{right-hand movements}}]/ 2$ (see Coles et al., 1988). In order to obtain a waveform for the NP condition, the N2cc/LRP complex was therefore obtained in relation to the response hand and not in relation to the hemifield of stimulus presentation. A first interval between 210 and 280 ms was considered, based on inspection of the grand averages, to determine the peak latency and amplitude of N2cc/LRP complex in the CP, IP and NP conditions. Absolute values were used in this analysis. We adopted the label "N2cc/LRP complex" although the N2cc component is absent in the NP condition. In a second interval, the peak latency of the LRP was measured in the CP, NP and IP conditions at between 300-500 ms with respect to the stimulus presentation. In this second interval the motor activity was expected to be free

of overlap from the N2cc component, according to the N2cc latency reported in previous studies, that is, about 150-200 ms (Leuthold and Schröter, 2006). The HEOG for the 3 conditions is shown in order to discard differences in ocular movements in the lateralized conditions (CP and IP) with respect to the NP.

N2pc and N2cc components were isolated from the motor activity related with the response through the next procedure: First, the direct waveforms were obtained in each condition (CP, IP, and NP). Second, the next subtractions were carried out at each electrode site: $CP_{\text{left-hand movements}} - NP_{\text{left-hand movements;}}$ $CP_{\text{right-hand movements}} - NP_{\text{right-hand movements}}$; $IP_{\text{left-hand movements}} - NP_{\text{left-hand movements;}}$ and $IP_{\text{right-hand movements}} - NP_{\text{right-hand movements.}}$ Thus, the common motor activity in CP and IP respect to NP was removed (this step resulted in the waveforms depicted in Figure 2.1). Third, the resulting waveforms ($CP\text{-}NP_{\text{left-hand movements}}$, $CP\text{-}NP_{\text{right-hand movements}}$, $IP\text{-}NP_{\text{left-hand movements}}$, and $IP\text{-}NP_{\text{right-hand movements}}$) were computed –separately for the CP-NP and for the IP-NP waveforms- through the next procedure: $[(C4–C3)_{\text{left-hemifield target stimulus}} + (C3–C4)]_{\text{right-hemifield target stimulus}}$/ 2 to obtain the N2cc in the Lateralized − Neutral Position waveforms (L-NP) (see Figure 2.1. and Figure 4.1.); $[(P8–P7)_{\text{left-hemifield target stimulus}} + (P7–P8)_{\text{right-hemifield target stimulus}}]$/ 2 to obtain the N2pc in the L-NP waveforms (see Figure 4.2.). The N2cc and N2pc peaks in these L-NP waveforms were determined in a temporal window of 150-300 ms based on inspection of the grand averages.

Figure 2 about here

Analyses were carried out with e-LORETA software, which estimated the source of activity underlying the brain activity recorded at the 49 scalp electrodes. The analysis compared the brain activity in the CP, IP and NP conditions in eight temporal intervals of 50 ms, from 150 to 550 ms post-stimulus. On the basis of the distribution of the scalp-recorded electric potential, exact low-resolution brain electromagnetic

tomography (eLORETA) software (publicly available free academic software, at http://www.uzh.ch/keyinst/loreta.htm) was used to compute the cortical three-dimensional distribution of current density. The eLORETA method is a distributed, linear-weighted minimum norm inverse solution. The weights endow the tomography with the property of exact localization to test point sources, accurately yielding located images of current density; albeit with low spatial resolution (i.e. neighbouring neuronal sources will be highly correlated). The method and the proof of its exact zero-error localization property are described by Pascual-Marqui (2007, 2009).

The related LORETA and sLORETA tomographic methods (Pascual-Marqui, 2002; Pascual-Marqui et al., 1994) have been validated in several studies combining LORETA with other more established location methods such as functional Magnetic Resonance Imaging (fMRI, Mulert et al., 2004; Vitacco et al., 2002), structural MRI (Pizzagalli et al., 2004; Worrel et al., 2000; Zumsteg et al., 2005), Positron Emission Tomography (PET, Dierks et al., 2000; Pizzagalli et al., 2004; Zumsteg et al., 2005) and invasive implanted electrode recordings (Zumsteg et al., 2006). The results of these studies also validate eLORETA, owing to its improved localization properties. The intracerebral volume is partitioned in 6239 voxels at a spatial resolution of 5mm. The eLORETA images therefore represent the electric activity at each voxel in neuroanatomic Montreal Neurological Institute (MNI) space as the exact magnitude of the estimated current density. Anatomical labels, Brodmann areas and MNI coordinates are also reported.

2.6. Statistical analysis

With the aim of determining possible behavioural differences related to the experimental conditions, repeated measures ANOVAs were carried out with an within-subject factor, Condition (three levels: CP, IP and NP), for the RTs and for the

percentage of errors (PE). Additionally, the test of Kolmogorov-Smirnov was carried out with the PE in order to test whether the parametric assumptions were fulfilled. The PE was analyzed through no parametric tests (tests of Friedman and Wilcoxon). One-sample Student's t tests were used for each quintile intersection points (q1, q2, q3, q4), with the aim of determining if the interference (IP – CP and IP – NP) or facilitation effect (NP – CP) was significant in each of them. Also, with the aim of determining if the magnitude of the interference or facilitation varied in relation to the speed of response, a repeated measures ANOVA was carried out with one within-subject factor: Quintile Intersection Points (four levels: q1, q2, q3, q4).

A repeated measures ANOVA with one within-subject factor, Condition (three levels: CP, NP and IP), was applied to the peak latencies of the LRP. Repeated measures ANOVAs with one within-subject factor, Condition (three levels: CP, IP and NP) were applied to N2cc/LRP complex and LRP peak latencies and amplitudes. Repeated measures ANOVAs with two within-subject factors, Condition (two levels: CP and IP) and Electrode (two levels: P7/8 and PO7/8), were carried out for the amplitude and latency of the N2pc.

With the Lateralized (CP and IP) minus Neutral Position waveforms (L-NP) repeated measures ANOVAs for peak latency and peak amplitude were carried out with two within-subject factors, Condition (two levels: CP – NP and IP – NP) and Electrode (two levels: C3/4 and P7/8). These analyses are carried out in the same repeated measures ANOVA with the aim of showing the functional dissociation between the components N2pc (measured at P7/8 electrode sites) and N2cc (measured at C3/4 electrode sites). Furthermore, to study whether the N2cc was significant in the CP condition one-sample t-tests were carried out on the average amplitude in ± 25 ms around the maximum negative peak observed in the CP condition in a 150-300 ms

temporal window (see Figure 4.1). In order to demonstrate that N2cc was constituted by activity in the hemisphere contralateral to the hemifield where the stimulus was presented (N2cc activity) and not by activity contralateral with respect to the hand that executed the response (which would represent motor activity not subtracted), one-sample t-test was carried out on the waveforms of the set of subtractions depicted in the Figure 2.1. The t-tests were carried out on the average amplitude in the temporal window where the N2cc was larger in the IP condition (220-270 ms, see Figure 4.1).

The Greenhouse-Geisser ε correction for the degrees of freedom was performed where necessary and the corresponding α levels are given. When the ANOVAs revealed significant effects due to the factors and their interactions, post-hoc multiple pairwise comparisons of the mean values were carried out (with Bonferroni corrections).

The eLORETA software was used to perform voxel-by-voxel within-subject comparisons for each of the 50 ms intervals analyzed (see Data Analysis), in order to identify possible differences in the brain electrical activity between pairs of conditions (CP and NP; IP and NP; CP and IP). Non-parametric statistical analysis of functional eLORETA images (Statistical non-Parametric Mapping; SnPM) was performed with a log-F-ratio statistic for paired groups. The results correspond to maps of log-F-ratio statistics for each voxel, for corrected $p < 0.05$. As explained in the review by Nichols and Holmes (2002), the SnPM methodology corrects for all multiple comparisons and does not require any assumption of Gaussianity.

3. Results

3.1. Behavioural Measures

The repeated measures ANOVA (Condition) revealed a significant effect of the factor on the RT ($F(2,36) = 53.0$, $p < 0.001$), as the RT was shorter in CP trials ($p < 0.001$) and NP trials ($p < 0.001$) than in IP trials, and on the percentage of errors (PE) ($F(2,36) =$

18.6, $p < 0.001$), as the PE was greater in IP trials than in CP trials ($p = 0.002$), and in NP ($p < 0.001$) (see Table 1). The assumptions for parametric testing were fulfilled for the CP and IP conditions although not for the NP condition: for the CP condition (KS (19) = 0.185, $p = 0.085$); IP condition (KS (19) = 0.121, $p = 0.200$); NP condition (KS (19) = 0.121, $p = 0.014$). Therefore, the no parametric test of Friedman was carried out, revealing the existence of significant differences between experimental conditions ($F(2,19) = 14.00$, $p = 0.001$). Additionally, the no parametric test of Wilcoxon was carried out, revealing that the existence of significant differences occurred between the IP and the CP condition ($Z = -3.059$, $p = 0.002$) and between the IP and the NP condition ($Z = -3.501$, $p < 0.001$).

With regard to the magnitude of the interference (in IP-CP: q1 = 36 ms; q2 = 43 ms; q3 = 43 ms; q4 = 40 ms; and in IP-NP: q1 = 43 ms; q2 = 42 ms; q3 = 43 ms; q4 = 50 ms), the one-sample t-tests revealed that the Simon effect was significant for the 4 quintile intersection points in IP – CP: q1 ($t(18) = 7.22$, $p < 0.001$); q2 ($t(18) = 8.53$, $p < 0.001$); q3 ($t(18) = 8.21$, $p < 0.001$) and q4 ($t(18) = 4.76$, $p < 0.001$), as well as in IP – NP: q1 ($t(18) = 6.84$, $p < 0.001$); q2 ($t(18) = 8.44$, $p < 0.001$); q3 ($t(18) = 6.29$, $p < 0.001$) and q4 ($t(18) = 5.52$, $p < 0.001$). The repeated measures ANOVA (Quintile Intersection Point) did not reveal any significant factor effects. With regard to the magnitude of facilitation (NP-CP: q1 = -7 ms; q2 = 1 ms; q3 = 1 ms; q4 = -10 ms), neither the t tests nor the repeated measures ANOVA (Quintile Intersection Points) revealed any significant effect.

Table 1 about here

3.2. ERP

With respect to the N2cc/LRP complex peak latency, the repeated measures ANOVA (Condition) did not reveal any significant effect of the factor. With respect to the

N2cc/LRP complex peak amplitude, the repeated measures ANOVA (Condition) revealed a significant effect of the factor ($F(1,14) = 26.3$, $p < 0.001$), as the amplitude was larger in the CP than in the IP condition ($p < 0.001$) and in the NP than in the IP condition ($p < 0.001$) (see Table 1).

The repeated measures ANOVA (Condition) for the LRP peak latency - measured at the second interval, 300-500 ms (see Data Analysis) - revealed a significant effect of the factor ($F(2,28) = 8.0$, $p = 0.002$), as the latencies were shorter in the CP than in the IP condition ($p = 0.048$) and shorter in the NP than in the IP condition ($p = 0.013$) (see Table 1). Note that between 300-500 ms the motor activity did not overlap with the N2cc component since at this time in L-NP subtractions, the waveforms (for CP-NP and IP-NP) are around baseline (see Figure 4).

The repeated measures ANOVA (Condition x Electrode) for the N2pc latency did not reveal any significant effect. With regard to the N2pc amplitude, the repeated measures ANOVA (Condition x Electrode) revealed a significant effect due to the Condition x Electrode interaction ($F(1,14) = 6.1$, $p = 0.027$), as the amplitude was larger at P7/8 than at PO7/8 ($p = 0.006$) in the CP condition.

Figure 3 about here

The repeated measures ANOVA (Condition x Electrode) for the peak latencies of lateralized minus neutral position (L-NP) waveforms did not reveal any significant effect. The repeated measures ANOVA (Condition x Electrode) for the amplitudes of L-NP waveforms revealed a significant effect of Electrode ($F(1,14) = 14.2$, $p = 0.002$), as the amplitude was greater in the P7/8 than in the C3/4 electrode pair ($p=0.002$). An effect of the Condition x Electrode interaction was also revealed ($F(1,14) = 7.8$, $p = 0.014$), as the amplitude was greater in the IP than in the CP condition at the C3/4

electrode pair (p = 0.004), while there were no such differences at the P7/8 electrode pair.

Figure 4 about here

The one-sample t-test carried out on the mean amplitude around the larger negative peak in the CP condition of the L-NP waveforms was significant: t (14) = -5.845, p < 0.001. With regard the analyses carried out, in the N2cc time interval (220-270 ms), in order to demonstrate that N2cc in the incompatible L-NP waveform was constituted by activity in the hemisphere contralateral to the hemifield where the stimulus was presented (N2cc activity) and not by activity contralateral with respect to the hand that executed the response, the one sample t-tests revealed no significant differences against zero in the electrodes contralateral to the hand movement: $IP_{\text{left-hand movements}} - NP_{\text{left-hand movements}}$ at C4 (t (14) = -1.504, p = 0.155); $IP_{\text{right-hand movements}} - NP_{\text{right-hand movements}}$ at C3 (t (14) = 0.891, p = 0.388). On the other hand, the one sample t-tests showed significant differences against zero in the electrodes contralateral to the position of the stimuli: $IP_{\text{left-hand movements}} - NP_{\text{left-hand movements}}$ at C3 (t (14) = -4.216, p = 0.001); $IP_{\text{right-hand movements}} - NP_{\text{right-hand movements}}$ at C4 (t (14) = -1.922, p = 0.075).

3.3. eLORETA

The brain regions in which the SnPM log-F-ratio statistic for paired groups was statistically significant are listed, along with the MNI coordinates, in Table 2. The regions in which the brain activity differed between conditions are shown in Figure 5.

In the 150-200 ms interval, the activity was greater in the CP than in NP condition (log-F-ratio = 1.3, p = 0.034), and in IP than in NP condition (log-F-ratio = -1.0, p = 0.006) in premotor areas.

In the 200-250 ms interval the activity was greater in the CP than in NP condition, mainly in Brodmann areas 5 and 7 (log-F-ratio = 1.1, p = 0.018) (see Table 2 and Figure 5).

Table 2 and Figure 5 about here

4. Discussion

In the present study a Simon effect was obtained (longer Reaction Time, RT, in the incompatible position (IP) than in the compatible position (CP)). Consistent with the Simon effect, LRP peak latency was longer in the IP than in the CP condition. Lateralized minus Neutral position (L-NP) waveforms showed larger N2cc amplitude in the IP than in the CP condition. It indicated that greater resources were engaged for monitoring the selection of the response in IP than in CP. The eLORETA analysis revealed more premotor activity in CP and IP -where N2cc activity was expected to appear- than in NP, in a temporal window between 150 and 200 ms. Otherwise N2pc did not show any differences according to the experimental manipulation, providing new evidence of functional dissociation between N2pc and N2cc components.

The behavioural results revealed a Simon effect due to stimulus-response interference in the IP condition, manifested by a longer reaction time (RT) and a higher percentage of errors (PE) in the IP condition than in the CP and in the NP conditions. These results are consistent with those of previous studies (see Lu and Proctor, 1995). A facilitation effect was absent since there were no significant differences between the NP and CP conditions in the RT, PE, DA and LRP measures. The absence of differences between CP and NP in the different measures also indicates that the different eccentricity of both stimuli did not affect the performance. Moreover, the HEOG showed an absence of differences between the three conditions of the task in ocular

movements in response to the stimulus position, probably because of the short time of stimuli presentation, as suggested by Abrahamse and Van der Lubbe (2008).

With respect to electrophysiological measures, longer LRP peak latency was observed in IP than in CP condition, which is consistent with the RT and with the results of previous studies (Praamstra and Plat, 2001). Although the onset of the correct response cannot be measured in horizontal arrangements due to the N2cc/LRP overlap, studies that used vertical arrangements of stimuli and responses (de Jong et al., 1994; Stürmer et al., 2002; Valle-Inclán, 1996, Experiment 3) established the interference locus in the response selection. However, as explained below, the horizontal arrangement of the stimuli enabled better comprehension of the effects of stimulus position on the visuospatial processing of the relevant stimulus and the cognitive control to monitor the tendency of response based on the stimulus position, i.e. the processes related to N2pc and N2cc.

In the present study, the motor activity was removed through the L-NP waveforms with the purpose of studying how N2cc and N2pc components are modulated on the basis of whether the stimulus position is compatible or incompatible with the response. In these L-NP waveforms, N2pc did not present any modulation related to the experimental manipulation. It supported that the Simon effect does not occur in the visuospatial processing of the relevant stimulus (Praamstra and Oostenveld, 2003; Van der Lubbe and Verleger, 2002). In relation with these findings, eLORETA analysis showed greater activity in Brodmann areas 5 and 7 within the interval 200-250 ms in CP than in NP. Although such differences in activation were absent between IP and NP, they may be related to the N2pc component that is present in the CP but absent in the NP condition (Luck and Hillyard, 1994; Woodman and Luck, 1999, 2003).

The N2cc amplitude was larger in IP-NP than in CP-NP, which is consistent with greater activity associated to the cognitive control of the response in the IP than in the CP condition. Even so, t-test revealed that the N2cc amplitude was significantly larger than zero in the CP condition (Figure 4.1). Also, eLORETA analysis revealed greater activity in premotor regions in CP and IP than in the NP condition between 150 and 200 ms. That activity seems related to the N2cc component since it was observed in the spatially lateralized conditions (CP and IP) in which N2cc was expected to appear. Also, although the results should be taken cautiously, due to the low spatial resolution of the eLORETA, the activity occurs in a region consistent with the sources of N2cc, the premotor cortex (see Praamstra and Oostenveld, 2003), within the temporal window in which N2cc was expected to appear (Leuthold and Schröter, 2006), although it was more coincident with the L-NP onset than with the L-NP peak.

Some caveats inherent to the subtraction procedures were pointed out (see Van Boxtel, 2004). Specifically, the new waveforms obtained through subtraction procedures usually derivate from differences in latency or amplitude from the constituent waveforms. Thus, the L-NP waveforms might have resulted from differences in motor activity not subtracted between CP and IP with respect to the NP condition leading to misleading interpretations. However, no differences were found between CP and NP in behavioural (RT, PE and DA) and electrophysiological parameters (LRP peak latency) related to motor activity. Thus, there are reasons to consider that motor activity was removed through the CP-NP subtraction. Therefore, the L-NP waveform observed in the CP condition as well as the differences revealed by eLORETA in the CP vs. NP comparison may be due to the N2cc, which is present in the CP but not in the NP condition where the stimuli are not spatially lateralized.

With respect to possible residual motor activity in the IP-NP subtraction, differences were showed in RT throughout the distribution of RTs. Also, a larger positivity for IP than NP was mainly present between 200-300 ms (see Figure 3.1). This positivity could be due to the preparation of the incorrect response and / or subsequent delay in preparing the correct movement in IP with respect to NP. If so, it would contaminate the L-NP waveform in the IP condition due to residual motor activity still present after-subtraction. To study this possibility t-tests on the first set of subtractions (Figure 2.1) were carried out for electrodes C3 and C4 on the average amplitude between 220-270 ms, where larger N2cc was observed in the L-NP waveform. The t-tests showed that the IP-NP subtraction resulted in not significant waveform in central contralateral electrodes to the hand of the response. Contrarily, significant negativity after-subtraction was observed in contralateral electrodes with respect to the hemifield of presentation of the stimulus. Thus, the L-NP waveform in the IP condition was the sum of the corresponding negativities contralateral to the hemifield of presentation of the stimuli.

It could be argued that a preparation of the incorrect response in the IP is still present in the L-NP waveform, since it would be absent in NP. In fact, the positive wave observed in the IP condition through the LRP derivation–see Figure 3.1- is closely similar to the wave associated to preparation of the incorrect response in vertical Simon tasks (Valle-Inclán, 1996, Exp. 3). However, such positive wave has been just related with the N2cc component in horizontal Simon tasks (Praamstra, 2006). Praamstra (2006) compared one horizontal Simon task where the participants responded to the stimuli as soon as it were presented in the screen with other horizontal Simon task where the response were hold back until the appearance of a signal. Considering the functional role of N2cc -to prevent the cross-talk between the direction of the spatial

attention and the manual response preparation (Praamstra and Oostenveld, 2003) - in the second task activity underlying to N2cc was not necessary since attentional shift to the stimulus position and manual response preparation occurred at different times. Although the effect of interference was similar in both tasks only in the first task the positive wave in the incompatible condition was present. It evidenced that such positivity was related to N2cc activity and not to preparation of the incorrect response, which in addition was supported by dipole source models data (Praamstra, 2006).

The lateralization of the premotor activity revealed by eLORETA to the left hemispheric is consistent with differences between both conditions in the N2cc component. Previous studies suggested that the left hemisphere contribute more than the right hemisphere to the N2cc (Praamstra and Oostenveld, 2003). Also it is consistent with the lateralization of the dPM in monitoring selection of responses: the left hemisphere lesions have a disruptive effect on the ability of patients to select between movements according to arbitrary rules (Rushworth et al., 1998). In addition, transcranial magnetic stimulation (TMS) to the left PMd disrupts the selection of movements that will be made by either hand (Johansen-Berg et al., 2002; Schluter et al., 1998).

In accordance with the activity observed in the premotor cortex, other studies using techniques with higher spatial resolution, e.g. PET and fMRI (Corbetta et al., 1993; Gitelman et al., 1999; Rosen et al., 1999), have shown that the premotor cortex is activated by attentional changes. Furthermore, fMRI studies specifically focused on the Simon effect have detected activation in the dorsal premotor cortex (Petersen et al., 2002; Wittfoth et al., 2006) and in the supplementary motor area (Liu et al., 2004; Wittfoth et al., 2006), which the authors attributed to resolution of the conflict.

The evidence from L-NP supports that N2cc activity is greater in IP than in CP condition. Therefore, these results support the suggestion of N2cc as a mechanism involved in monitoring the selection of the response (Praamstra and Oostenveld, 2003). In the IP condition greater effort would be necessary to select the appropriate response since it do not coincide with the compatible spatially response. This greater effort would be related with larger activity related to N2cc. Stürmer and Leuthold (2003) proposed an ancillary mechanism monitoring (AMM) in Simon tasks, which would be responsible to monitoring the response selection and selectively suppresses output of the unconditional route whereby location-based signals are prevented from accessing the motor system. The present results are in line with the suggestion of Leuthold and Schröter (2006) of the N2cc component representing such mechanism of cognitive control.

Moreover, the present results obtained by means of the L-NP subtractions add new support for the functional dissociation between N2cc and N2pc (Praamstra, 2006; Praamstra and Oostenveld, 2003), as differences in amplitude between conditions were found for N2cc but not for N2pc. This functional dissociation is consistent with the findings of some studies that identified different foci of activity associated with N2pc and N2cc (Oostenveld et al., 2001; Praamstra and Oostenveld, 2003; Praamstra and Plat, 2001).

The present study used a horizontal arrangement of stimuli and responses whereby the measure of the covert response activation (LRP onset) was sacrificed in benefit of the study of N2pc and N2cc components, since the N2cc plays an important role in spatial stimulus-response compatibility tasks that are worthy of further research, as concluded in the review by Leuthold (2011). As far as we are concerned, the present results showed for the first time that N2cc activity was higher when the stimulus

position was spatially incompatible than when it was spatially compatible with the required response. The N2cc component may therefore be a useful tool for evaluating populations in which deficits in spatial response inhibition are expected to occur.

5. Conclusions

In the present study, the motor activity was eliminated through L-NP subtractions, which revealed larger N2cc amplitude in IP than in CP, in accordance with the greater effort required to monitor the selection of the correct response in the IP condition. Additional information about N2cc was provided by eLORETA analysis, which revealed greater premotor activity between 150 and 200 ms in IP and CP than in NP. The functional dissociation between N2pc and N2cc components was indicated by the fact that N2cc, but not N2pc, was differentially affected by the experimental condition.

Acknowledgements

This work was financially supported by funds from the Spanish Ministerio de Educación (Beca FPU AP2007-04362; SEF2007- 67964-C02-02; PSI2010-22224-C03-03), and from the Galician Government: Consellería de Industria e Innovación /Economía e Industria (PGIDIT07PXIB211018PR, 10 PXIB 211070 PR); and Consellería de Educación e Ordenación Universitaria (Axudas para a Consolidación e Estruturación de unidades de investigación competitivas do sistema universitario de Galicia. Modalidade: Redes Novas. Expediente: 2010/56 -with FEDER funds-).

REFERENCES

Abe, M., Hanakawa, T., 2009. Functional coupling underlying motor and cognitive functions of the dorsal premotor cortex. Behav. Brain Res. 198, 13-23.

Abrahamse, E., Van der Lubbe, R., 2008. Endogenous orienting modulates the Simon effect: critical factors in experimental design. Psychol. Res. 72 (3), 261-272.

Bargh, J.A., Chartrand, T.L., 2000. The mind in the middle: a practical guide to priming and automaticity research. In: Reis, H.T., Hudd C.M. (Eds.), Handbook of research methods in social psychology, Cambridge UK: Cambridge University Press, pp. 253-285.

Coles, M.G., Gratton, G., Donchin, E., 1988. Detecting early communication: using measures of movement-related potentials to illuminate human information processing. Biol. Psychol. 26, 69-89.

Corbetta, M., Miezin, F.M., Shulman, G.L., Petersen, S.E., 1993. A PET study of spatial attention. J. Neurosci. 13, 1202-1226.

De Jong, R., Liang, C.C., Lauber, E., 1994. Conditional and unconditional automaticity: a dual-process model of effects of spatial stimulus-response correspondence. J. Exp. Psychol. Hum. Percept. Perform. 20 (4), 731.

Dierks, T., Jelic, V., Pascual-Marqui, R.D., Wahlund, L., Julin, P., Linden, D.E., Maurer, K., Winblad, B., Nordberg, A., 2000. Spatial pattern of cerebral glucose metabolism (PET) correlates with localization in intracerebral EEG-generators in Alzheimer's disease. Clin. Neurophysiol. 111, 1817-1824.

Eimer, M., 1998. The lateralized readiness potential as an on-line measure of selective response activation. Behav. Res. Methods Instrum. Comput. 30, 146-156.

Galashan, D., Wittfoth, M., Fehr, T., Herrmann, M., 2008. Two Simon tasks with different sources of conflict: An ERP study of motion- and location-based compatibility effects. Biol. Psychol. 78, 246-252.

Gitelman, D. R., Nobre, A.C., Parrish, T.B., LaBar, K.S., Kim, Y.H., Meyer, J.R., Mesulam, M., 1999. A large-scale distributed network for covert spatial attention:

Further anatomical delineation based on stringent behavioural and cognitive controls. Brain, 122, 1093-1106.

Gratton, G., Coles, M.G.H., Donchin, E., 1983. A new method for off-line removal of ocular artefact. Electroencephalogr. Clin. Neurophysiol. 55, 468-484.

Gratton, G., Coles, M.G.H., Sirevaag, E.J., Eriksen, C.W., Donchin, E., 1988. Pre-and poststimulus activation of response channels: a psychophysiological analysis. J. Exp. Psychol. Hum. Percept. Perform. 14 (3), 331-344.

Johansen-Berg H, Rushworth MF, Bogdanovic MD, Kischka U, Wimalaratna S, Matthews PM., 2002. The role of ipsilateral premotor cortex in hand movement after stroke. Proc. Natl. Acad. Sci. 99, 14518-14523.

Kornblum, S., Stevens, G., 2002. Sequential effects of dimensional overlap: findings and issues. In: Prinz, W. (Ed.), Common Mechanism in Perception and Action. Oxford Univ. Press, Oxford, pp. 9-54.

Leuthold, H., 2011. The Simon effect in cognitive electrophysiology: a short review. Acta Psychol. 136, 203-211.

Leuthold, H., Schröter, H., 2006. Electrophysiological evidence for response priming and conflict regulation in the auditory Simon task. Brain Res. 1097, 167-180.

Liu, X., Banich, M.T., Jacobson, B.L., Tanabe, J.L., 2004. Common and distinct neural substrates of attentional control in an integrated Simon and spatial stroop task as assessed by event-related fMRI. Neuroimage, 22, 1097-1106.

Lu, C.H., Proctor, R.W., 1995. The influence of irrelevant location information on performance: A review of the Simon and spatial Stroop effects. Psychon. Bull. Rev. 2, 174-207.

Luck, S.J., Hillyard, S.A., 1994. Spatial filtering during visual search: Evidence from human electrophysiology. J. Exp. Psychol. Hum. Percept. Perform. 20, 1000-1014.

Mancebo-Azor, R., Sáez-Moreno, J.A., Domínguez-Hidalgo, I., Luna-Del Castillo, J.D., Rodríguez-Ferrer, J.M., 2009. Efectos del contraste, excentricidad y posición en la detección de estímulos visuales en humanos. Rev. Neurol. 48 (3), 129-133.

Mulert, C., Jäger, L., Schmitt, R., Bussfeld, P., Pogarell, O., Möller, H.J., Juckel, G., Hegerl, U., 2004. Integration of fMRI and simultaneous EEG: toward a comprehensive understanding of localization and time-course of brain activity in target detection. Neuroimage, 22, 83-94.

Nichols, T.E., Holmes, A.P., 2002. Nonparametric permutation test for functional neuroimaging: a primer with examples. Hum. Brain Mapp. 15, 1-25.

Oldfield, R.C., 1971. The assessment and analysis of handedness: the Edinburgh inventory. Neuropsychologia, 9, 97-113.

Oostenveld, R., Praamstra, P., Stegeman, D.F., Van Oosterom, A., 2001. Overlap of attention and movement-related activity in lateralized event-related brain potentials. Clin. Neurophysiol. 112, 477-484.

Pascual-Marqui, R.D., 2002. Standarized low-resolution brain electromagnetic tomography (Sloreta): technical details. Meth. Find. Exp. Clin. Pharmacol. 24 (Suppl. D.), 5-12.

Pascual-Marqui, R.D., 2007. Discrete, 3D distributed, linear imaging methods of electric neuronal activity. Part 1. Exact zero error localization. arXiv: 0710.3341 [math-ph], http://arxiv.org/pdf/0710.3341.

Pascual-Marqui, R.D., 2009. Theory of the EEG inverse problem. In: Tong, S., Thakor, N. (Eds.), Quantitative EEG analysis: methods and applications. Artech House, Boston, pp. 121-140.

Pascual-Marqui, R.D., Michel, C.M., Lehmann, D., 1994. Low resolution electromagnetic tomography: a new method for localizing electrical activity in the brain. Int. J. Psychophysiol. 18, 49-65.

Petersen, B.S., Kane, M.J., Alexander, G.M., Lacadie, C., Skudlarski, P., Leung, H.-C., May, J., Gore, J. C., 2002. An event-related functional MRI comparing interference effects in the Simon and Stroop tasks. Cogn. Brain Res. 13, 427-440.

Pizzagalli, D.A., Oakes, T.R., Fox, A.S., Chung, M.K., Larson, C.L., Abercrombie, H.C., Schaefer, S.M., Benca, R.M., Davidson, R.J., 2004. Functional but not structural subgenual prefrontal cortex abnormalities in Melancholia. Mol. Psychiatry 9 (325), 393-405.

Praamstra, P., 2006. Prior information of stimulus location: Effects on ERP measures of visual selection and response selection. Brain Res. 1072, 153-160.

Praamstra, P., 2007. Do's and don'ts with lateralized event-related brain potentials. J. Exp. Psychol. Hum. Percept. Perform. 33 (2), 497-502.

Praamstra, P., Oostenveld, R., 2003. Attention and movement-related motor cortex activation: a high-density EEG study of spatial stimulus-response compatibility. Cogn. Brain Res. 16, 309-322.

Praamstra, P., Plat, F.M., 2001. Failed suppression of direct visuomotor activation in Parkinson's disease. J. Cogn. Neurosci. 13 (1), 31-43.

Rosen, A.C., Rao, S.M., Caffara, P., Scaglioni, A., Bobholz, J.A., Woodley, S.J., Hammeke, T.A., Cunningham, J.M., Prieto, T.E., Binder, J.R., 1999. Neural basis

of endogenous and exogenous orienting: A functional MRI study. J. Cogn. Neurosci. 11, 135-152.

Rubichi, S., Nicoletti, R., Iani, C., Umiltà, C., 1997. The Simon effect occurs relative to the direction of tan attention shift. J. Exp. Psychol. Hum. Percept. Perform. 23, 1353-1364.

Rushworth, M.F., Nixon, P.D., Wade, D.T., Renowden, S., Passingham, R.E., 1998. The left hemisphere and the selection of learned actions. Neuropsychologia, 36, 11-24.

Schluter, N.D., Rushworth, M.F., Passingham, R.E., Mills, K.R., 1998. Temporary interference in human lateral premotor cortex suggests dominance for the selection of movements. A study using transcranial magnetic stimulation. Brain, 121, 185-799.

Simon, J.R., 1990. Stimulus-response compatibility: An integrated perspective. In: Proctor, R.W., Reeve, T.G. (Eds.). The effects of an irrelevant directional cue on human information processing, North Holland, Amsterdam, pp. 31-88.

Stürmer, B., Leuthold, H., 2003. Control over response priming in visuomotor processing: a lateralized event-related potential study. Exp. Brain Res. 153, 35-44.

Stürmer, B., Leuthold, H., Soetens, E., Schröter, H., Sommer, W., 2002. Control over location-based response activation in the Simon task: behavioral and electrophysiological evidence. J. Exp. Psychol. Hum. Percept. Perform. 28 (6), 1345-1363.

Valle-Inclán, F., 1996. The locus of interference in the Simon effect: An ERP study. Biol. Psychol. 43 (2), 147-162.

Van der Lubbe, R.H.J., Jaśkowski, P., Wauschkuhn, B., Verleger, R., 2001. Influence of time pressure in a simple detection task, a choice-by-location task, and the Simon task. J. Psychophysiol. 15, 241-255.

Van der Lubbe, R.H.J., Verleger, R., 2002. Aging and the Simon task. Psychophysiology, 39(01), 100-110.

Van der Lubbe, R.H.J., Wauschkuhn, B., Wascher, E., Niehoff, T., Kömpf, D., Verleger, R., 2000. Lateralization with direction information for the preparation of saccades and finger movements. Exp. Brain Res., 132, 163-178.

Van Boxtel, G.J.M., 2004. The use of the subtraction technique in the psychophysiology of response inhibition and conflict. In: Ullsperger, M., Falkenstein, M. (Eds.), Errors, conflicts, and the brain. Current opinions on performance monitoring, Leipzig: Max Plank Institute Cognitive Neuroscience, pp. 219-225.

Vitacco, D., Brandeis, D., Pascual-Marqui, R., Marin, E., 2002. Correspondence of event-related potential tomography and functional magnetic resonance imaging during language processing. Hum. Brain Mapp. 17, 4-12.

Wascher, E., Wauschkuhn, B., 1996. The interaction of stimulus- and response-related processes measured by event-related lateralizations of the EEG. Electroencephalogr. Clin. Neurophysiol. 99, 149-162.

Wittfoth, M., Buck, D., Fahle, M., Herrmann, M., 2006. Comparison of two Simon tasks: neural correlates of conflict resolution based on coherent motion perception. Neuroimage, 32, 921-929.

Wise, G., S.P., Di Pelligrino, G., Boussaoud, D., 1996. The premotor cortex and nonstandard sensorimotor mapping. Can. J. Physiol. Pharmacol. 74, 469-482.

Wise, G., S.P., Boussaoud, D., Johnson, P. B., Caminiti, R., 1997. Premotor and parietal cortex: corticocortical connectivity and combinatorial computations. Annu. Rev. Neurosci. 20, 25-42.

Woodman, G.F., Luck, S.J., 1999. Electrophysiological measures of rapid shift of attention during visual search. Nature 400 (6747), 867-869.

Woodman, G.F., Luck, S.J., 2003. Serial deployment of attention during visual search. J. Exp. Psychol. Hum. Percept. Perform. 29 (1), 121-138.

Worrel, G.A., Lagerlund, T.D., Sharbrough, F. W., Brinkmann, B. H., Busacker, N. E., Cicora, K. M., O'Brien, T. J., 2000. Localization of the epileptic focus by low-resolution electromagnetic tomography in patients with a lesion demonstrated by MRI. Brain Topogr. 12, 273-282.

Zumsteg, D., Friedman, A., Wieser, H.G., Wenneberg, R.A., 2006. Propagation of interictal discharges in temporal lobe epilepsy: correlation of spatiotemporal mapping with intracranial foramen ovale electrode recordings. Clin. Neurophysiol. 117, 2615-2626.

Zumsteg, D., Wennberg, R.A., Treyer, V., Buck, A., Wieser, H.G., 2005. H2(15)O or 13NH3 PET and electromagnetic tomography (LORETA) during partial status epilepticus. Neurology, 65, 1657-1660.

FIGURE CAPTIONS

Figure 1. The task comprised six types of stimuli grouped in three conditions according to the position of the stimulus in relation to the hand making the response. The participants were instructed to respond by pressing the button on the left, with the left hand, when a blue arrow appeared, and the button on the right, with the right hand, when a red arrow appeared, while ignoring the stimulus position. The conditions presented from left to right were: compatible position (CP), neutral position (NP) and incompatible position (IP).

Figure 2. The procedure to obtain the L-NP is graphically represented for the IP condition. 2.1. In the first set of operations the "IP-NP" subtraction was carried out for the stimulus-related waveforms on each electrode individually. In this step the motor activity between IP and NP was removed in the N2cc interval resulting in a waveform around the baseline in the contralateral electrodes to the hand that executes the response (C3 for right hand movements and C4 for left hand movements). Moreover, the subtraction resulted in negative waveforms at contralateral electrodes to the stimulus presentation (C3 for stimuli presented on the right and C4 for stimuli presented on the left hemifield), which represents the activity related to N2cc. 2.2. In the second set of operations the activity at C3 and C4 electrodes was averaged through the LRP formula (in the text) in order to obtain a single waveform related to N2cc activity on each condition. The same procedure was employed to subtract the motor activity in the CP condition.

Figure 3; 3.1) N2cc/LRP (first interval) and LRP (second interval) - obtained in relation to the hand of the response at C3/4 electrodes pair - are shown for the compatible position (CP) (solid line), incompatible position (IP) (dashed line) and neutral position (NP) (dotted line). N2cc/LRP peak amplitude was smaller in the IP than in the CP and NP conditions because of the correct response preparation was present in the CP and NP conditions while it was delayed in the IP condition as showed longer LRP peak latency in the second interval in IP condition; 3.2) The N2pc -obtained in relation to the hemifield of stimulus presentation at P7/8 electrodes pair- revealed an absence of differences between the CP (solid line) and the IP (dashed line) conditions; 3.3) The

HEOG for CP (solid line), IP (dashed line) and NP (dotted line) conditions showed no differences in ocular movements to the stimulus position between the three conditions.

Figure 4. N2cc (top) and N2pc (bottom) waveforms are shown after removal of the motor activity through lateralized minus neutral position (L-NP) subtractions for the compatible position (CP) (solid line) and the incompatible position (dashed line) at the C3/4 and P7/8 electrodes pair respectively. 4.1) N2cc component showed larger amplitude in the IP than in the CP condition. This indicates that greater inhibitory control of the stimulus position was required in the IP, in order to prevent cross-talk between the direction of spatial attention and the manual response activation. 4.2) Differences in the N2pc component were absent between CP and IP conditions as the interference locus in the Simon effect is not present in the visuospatial processing of the relevant stimulus. Evidence of functional dissociation between both N2cc and N2pc components was obtained since they were affected differently by the experimental manipulation.

Figure 5. eLORETA tomographies with the regions that showed significantly higher activation in the comparisons between CP and NP, and between NP and IP. In the CP vs. NP comparison, greater activation for CP than for NP is indicated in yellow and red, between 150-200 ms (top) and 200-250 ms (middle). In the NP vs. IP comparison (bottom) a lower activation in the window 150-200 ms for NP than for IP is indicated in blue. Greater activation in premotor regions was observed in both the CP and IP conditions relative to the NP condition in the 150-200 ms interval.

Table 1

CONDITION	CP	NP	IP
RT	408 (41)	401 (46)	444 (43)
PE	4.9 (3.5)	3.3 (3.0)	11.0 (6.9)
N2cc/LRP peak latency	246 (19.5)	238 (22.1)	238 (22.2)
N2cc/LRP peak amplitude	2.9 (1.3)	2.4 (1.3)	1.1 (0.8)
LRP peak latency	358 (39)	349 (44)	415 (59)
N2pc peak latency	244 (18.9)		238 (13.9)
N2pc peak amplitude	-3.8 (2.6)		-4.1 (2.9)
N2cc peak latency (L-NP)	223.3 (33.5)		250.2 (40.9)
N2cc peak amplitude (L-NP)	-1.4 (1.3)		-3.1 (1.7)
N2pc peak latency (L-NP)	240.1 (40.5)		232.5 (18.7)
N2pc peak amplitude (L-NP)	-4.4 (3.1)		-4.3 (3.4)

Table 1- Mean and standard deviation, for each Condition (Compatible Position (CP), Neutral Position (NP), and Incompatible Position (IP)) of Reaction Time (in milliseconds); Percentage of Errors (PE); peak latency and peak amplitude of N2cc/LRP complex at C3/C4; peak latency of the LRP at C3/C4. For CP and IP conditions: N2pc peak latency and peak amplitude at P7/P8. Mean and standard deviation of Lateralized minus Central Stimulus subtractions (L-NP) (Compatible Position minus Neutral Position (CP-NP) and Incompatible Position minus Neutral Position (IP-NP)) of N2cc peak latency and peak amplitude at C3/C4; N2pc peak latency and peak amplitude at P7/P8.

Table 2

ANATOMICAL REGION (BA) NP vs. IP (150-200 ms)	MNI COORDINATES X Y Z	ANATOMICAL REGION (BA) CP vs. NP (150-200 ms)	MNI COORDINATES X Y Z	ANATOMICAL REGION (BA) CP vs. NP (200-250 ms)	MNI COORDINATES X Y Z
Precentral Gyrus (6)	-15 -20 70	Medial Frontal Gyrus (6)	-5 -30 70	Paracentral Lobule (5)	-5 -50 65
Superior Frontal Gyrus (6)	-20 -15 70	Paracentral Lobule (4)	5 -40 70	Postcentral Lobule (2)	-30 -40 70
Superior Frontal Gyrus (6)	-15 -15 70	Paracentral Lobule (4)	-5 -35 70	Precuneus (7)	-5 -50 60
Precentral Gyrus (6)	-10 -20 70	Paracentral Lobule (4)	5 -35 70	Postcentral Gyrus (5)	-10 -50 65
Precentral Gyrus (6)	-20 -20 70	Paracentral Lobule (4)	-5 -40 70	Postcentral Gyrus (2)	-30 -40 65
Medial Frontal Gyrus (6)	-5 -20 70	Postcentral Lobule (5)	5 -45 70	Postcentral Gyrus (5)	-5 -50 70
Medial Frontal Gyrus (6)	-10 -15 70	Postcentral Gyrus (5)	-5 -25 70	Precuneus (7)	-5 -55 65
Middle Frontal Gyrus (6)	-20 -15 65	Medial Frontal Gyrus (6)	5 -30 70	Precuneus (7)	-10 -50 60
Superior Frontal Gyrus (6)	-20 -10 70	Medial Frontal Gyrus (6)	0 -35 65	Postcentral Gyrus (7)	-5 -55 70
Medial Frontal Gyrus (6)	0 -25 65	Postcentral Lobule (5)	-5 -45 70	Postcentral Gyrus (5)	-10 -50 70
Medial Frontal Gyrus (6)	0 -25 65	Medial Frontal Gyrus (6)	0 -30 65	Postcentral Gyrus (7)	-10 -55 65
Medial Frontal Gyrus (6)	-5 -25 70	Paracentral Lobule (5)	5 -35 65	Postcentral Gyrus (7)	-10 -55 70
Medial Frontal Gyrus (6)	5 -25 60	Postcentral Gyrus (5)	-5 -50 70	Precuneus (7)	-5 -55 60
Precentral Frontal Gyrus (6)	-25 -15 70	Postcentral Gyrus (5)	10 -35 70	Postcentral Gyrus (5)	-30 -45 70
Medial Frontal Gyrus (6)	5 -25 65	Medial Frontal Gyrus (6)	5 -30 65	Postcentral Gyrus (5)	-25 -45 70
Medial Frontal Gyrus (6)	-5 -15 70	Medial Frontal Gyrus (6)	-5 -30 65	Postcentral Gyrus (2)	-25 -40 65
Medial Frontal Gyrus (6)	-5 -20 60	Paracentral Lobule (5)	0 -40 65	Postcentral Gyrus (7)	-15 -55 70
Superior Frontal Gyrus (6)	-15 -10 70	Paracentral Lobule (5)	5 -40 65	Postcentral Gyrus (2)	-25 -40 70
Medial Frontal Gyrus (6)	0 -30 60	Precentral Gyrus (4)	-15 -30 70	Precuneus (7)	-5 -50 55
Medial Frontal Gyrus (6)	5 -30 60	Postcentral Gyrus (4)	10 -35 70	Postcentral Gyrus (5)	-20 -50 70
Medial Frontal Gyrus (6)	0 -30 65	Precentral Gyrus (4)	10 -30 70	Precuneus (7)	-5 -55 55
Medial Frontal Gyrus (6)	-5 -30 65			Precuneus (7)	0 -55 65
Medial Frontal Gyrus (6)	5 -20 65			Postcentral Gyrus (5)	-25 -45 65
				Sub-Gyrus (40)	-25 -40 60
				Postcentral Gyrus (40)	-30 -40 60
				Precuneus (7)	-10 -50 55
				Postcentral Gyrus (7)	-15 -55 65
				Precuneus (7)	-10 -55 55
				Precuneus (7)	-15 -50 60
				Superior Parietal (5)	-20 -45 65
				Postcentral Gyrus (5)	5 -50 70
				Precuneus (7)	0 -55 60
				Postcentral Gyrus (5)	-5 -45 65
				Superior Parietal (7)	-20 -50 65
				Postcentral Gyrus (7)	-10 -60 70

Table 2. Cortical regions significantly activated (by means of eLORETA) in the paired comparisons between conditions. Left panel: NP vs. IP (150-200 ms); middle panel: CP vs. NP (150-200 ms); right panel: CP vs. NP (200-250 ms). BA: Brodmann area; MNI: Montreal Neurological Institute.

Figure 1

Click here to download high resolution image

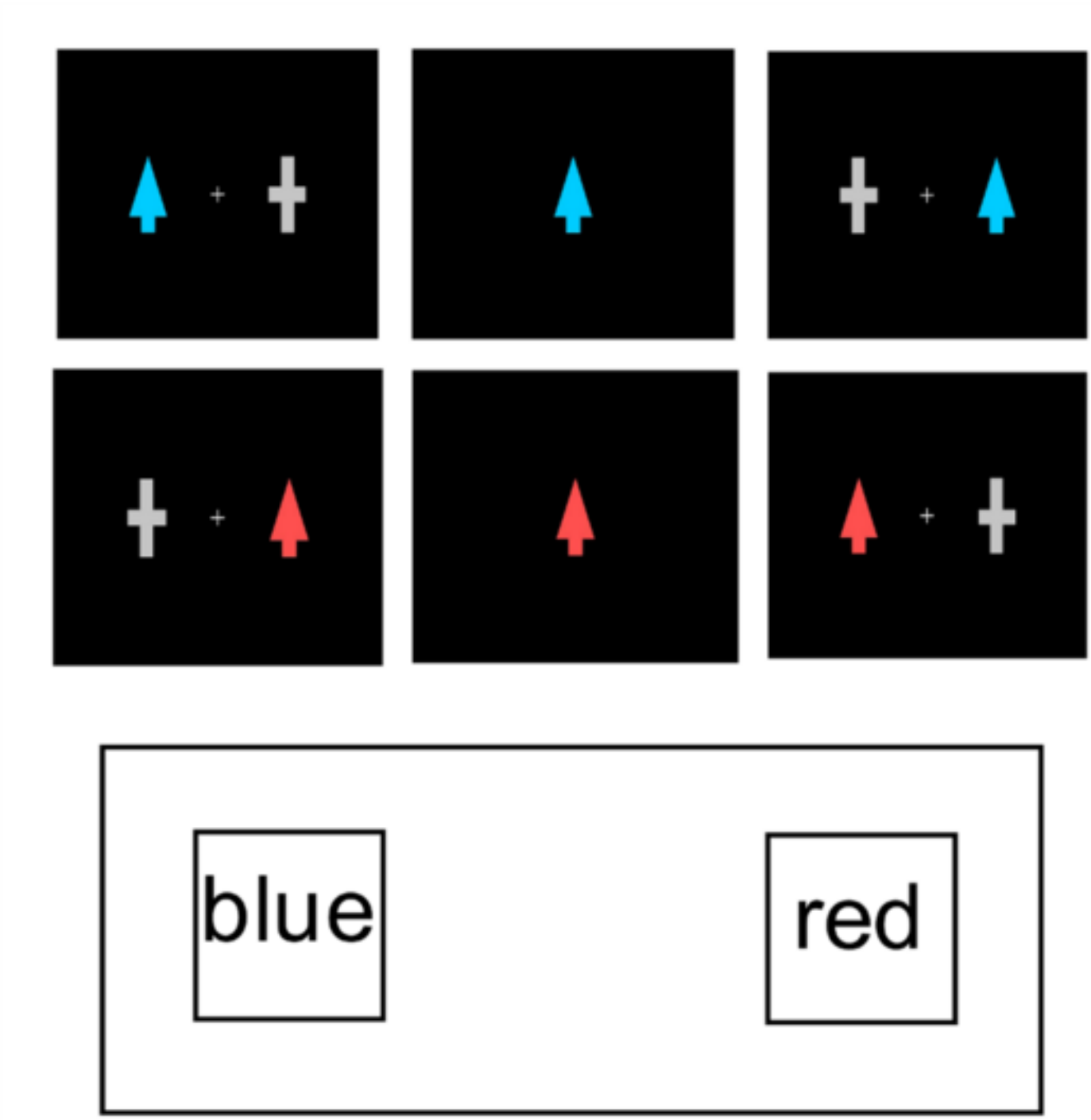

Figure 2
Click here to download high resolution image

2.1 Removing motor activity

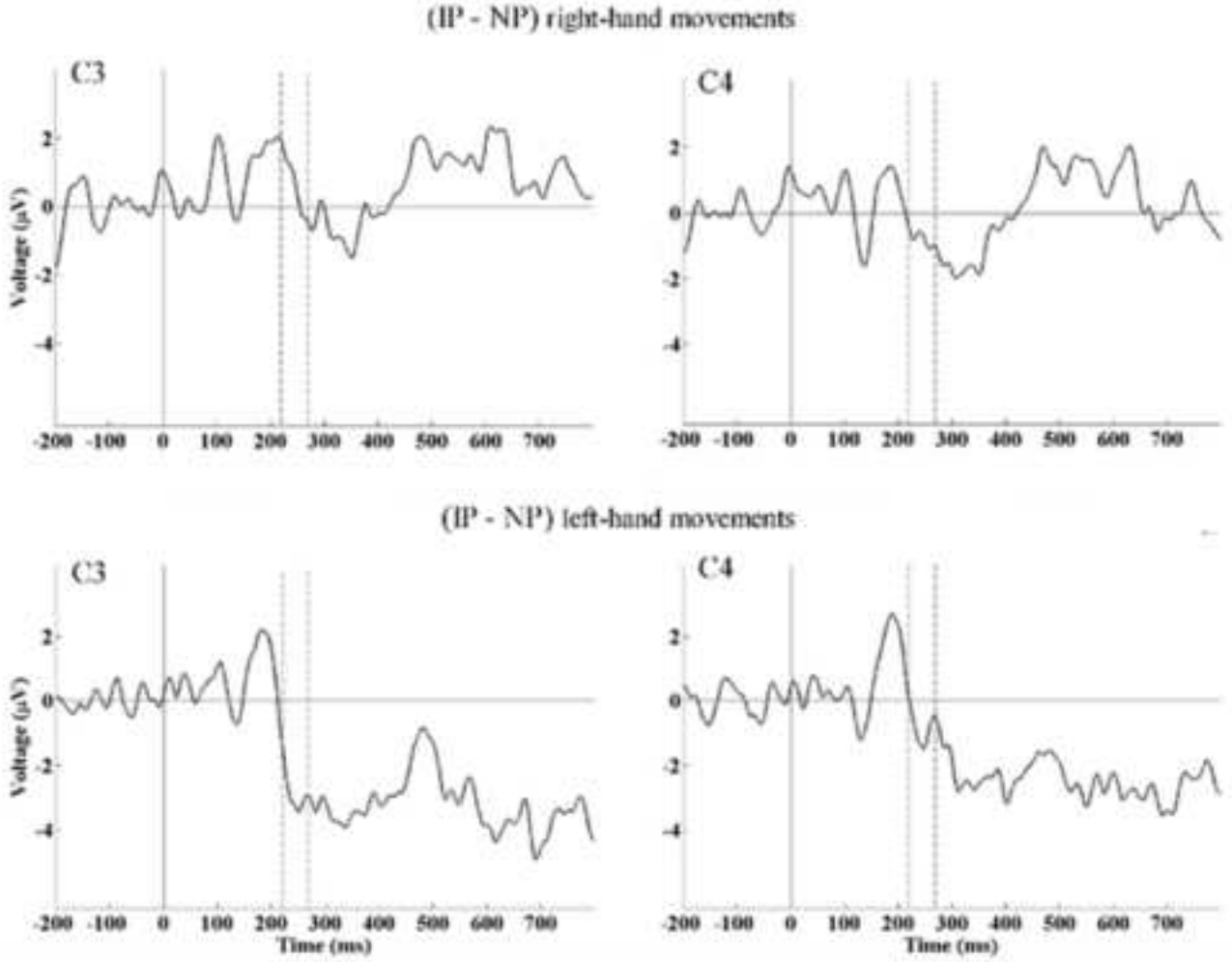

2.2 Averaging the waveforms

$$[(C4–C3)_{\text{left-hemifield target stimulus}} + (C3–C4)]_{\text{right-hemifield target stimulus}}]/\,2$$

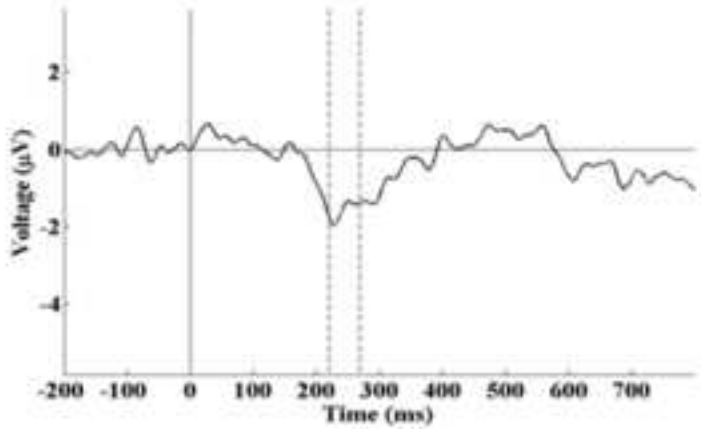

Figure 3

Click here to download high resolution image

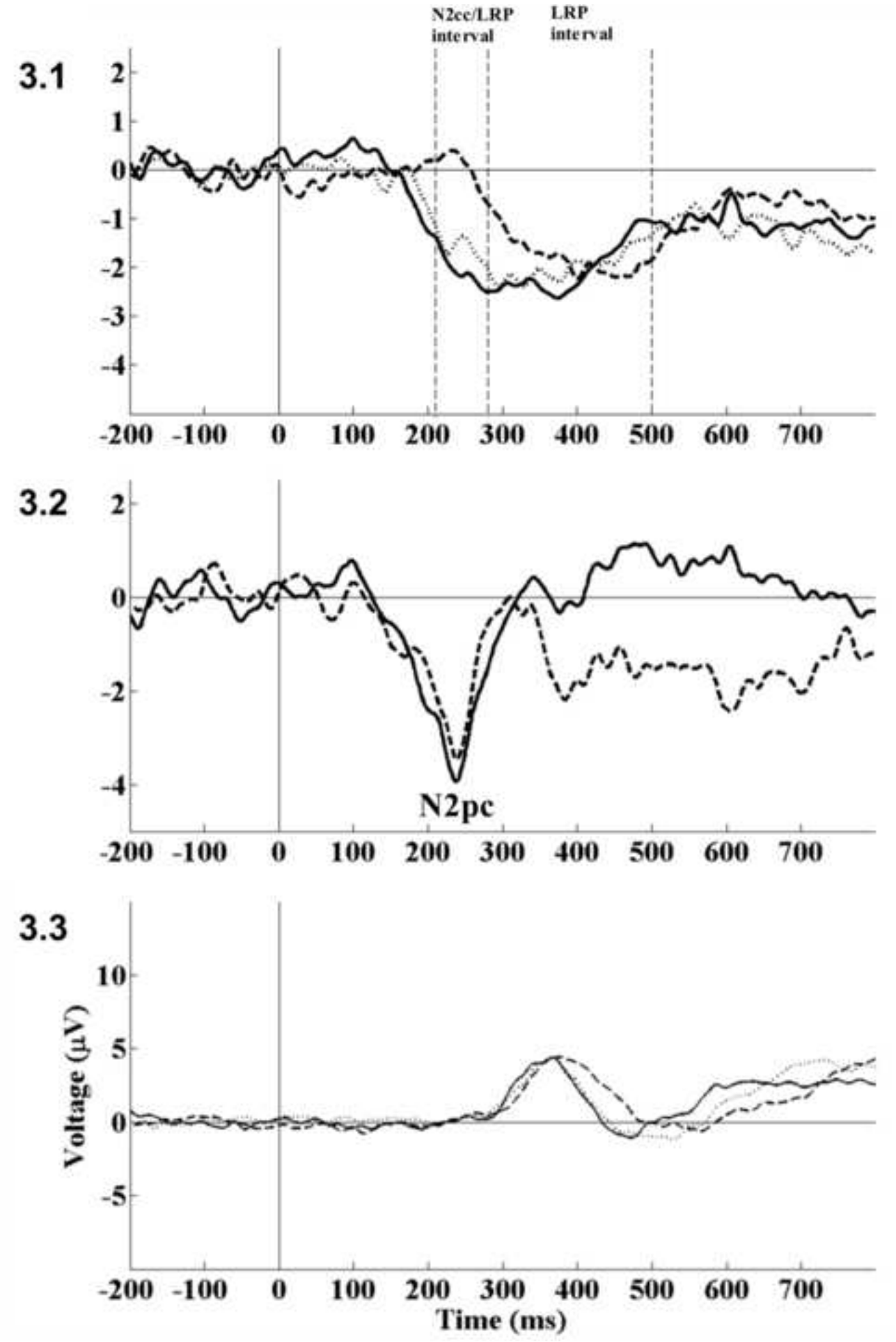

Figure 4
Click here to download high resolution image

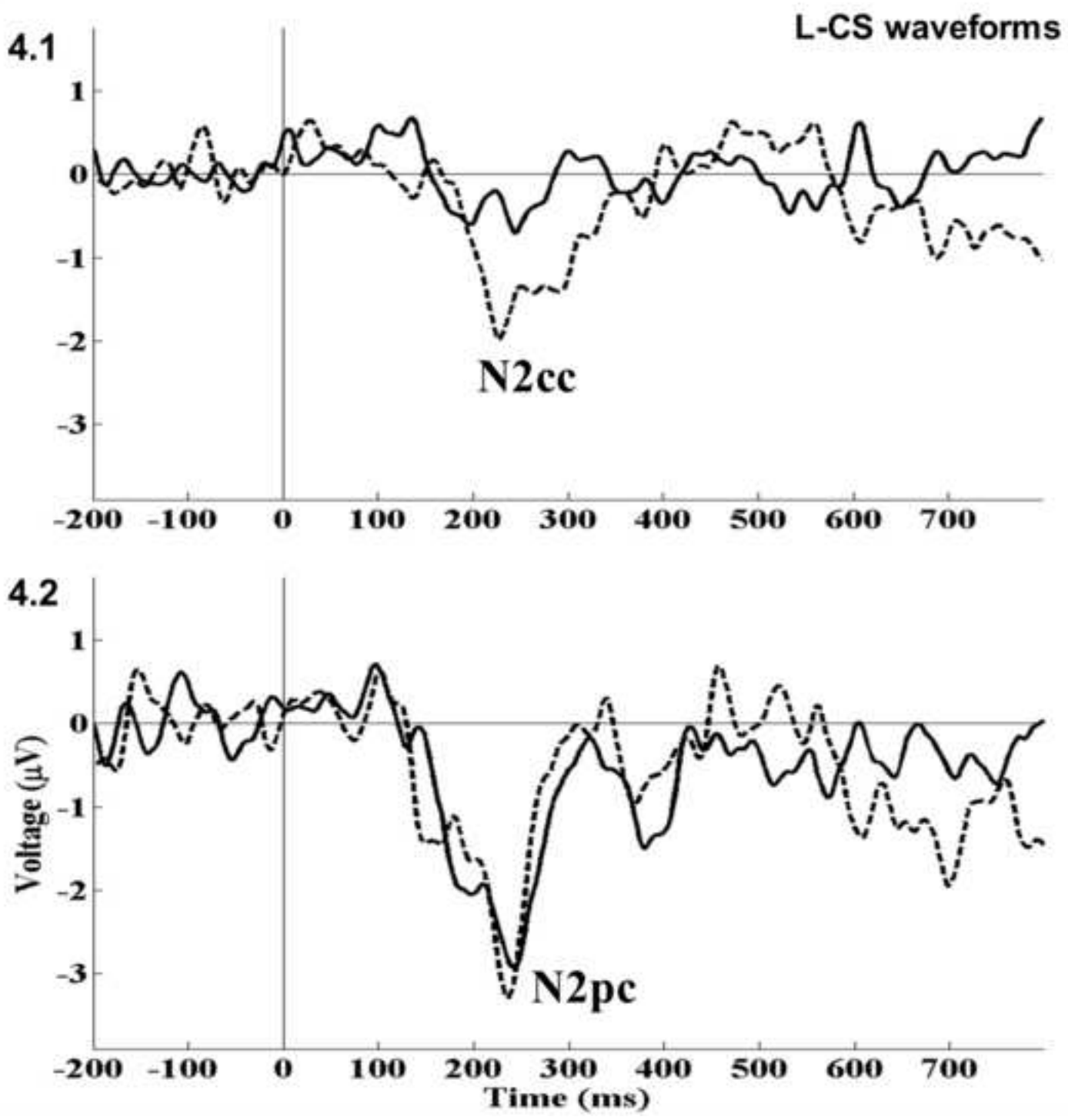

Figure 5

Click here to download high resolution image